T-stress determination using TSA and DIC

M. Zanganeh[1,a], R.A. Tomlinson[1,b] and J.R. Yates[1,c]

[1]University of Sheffield, Mechanical Engineering Department, Mappin Street, Sheffield, S1 3JD UK

[a]m.zanganeh@sheffield.ac.uk, [b]r.a.tomlinson@sheffield.ac.uk, [c]j.yates@sheffield.ac.uk

Keywords: T-stress, Thermoelastic stress analysis, Digital image correlation

Abstract. In this work T-stresses and intensity factors are determined experimentally using digital Image Correlation (DIC) and Thermoelastic Stress Analysis (TSA) in a DCB specimen. These techniques are assessed in a centre cracked specimen under different loading angles providing pure mode I, mixed mode I and II and pure mode II conditions. T-stresses have been found for these conditions and the effect of eccentricity in the loading on the results is discussed.

Introduction

In the simplest form of linear elastic fracture mechanics, it is assumed that the crack tip state is defined by using the singular term of the Williams' equation [1]. This approach has been used widely on many problems. However, it is not capable of fully interpreting some circumstances occurs. This was first demonstrated by Larsson and Carlsson [2] and later by Rice [3] by determining different plastic zone sizes and crack tip opening displacements for the same level of intensity factor applied a different crack geometries. They managed to verify their results by using a modified boundary layer formulation and considering the effect of the non-singular term, T-stress, in Williams' expansion.

The T-stress, which is the constant term in Williams' asymptotic expansion, is a non-singular stress which acts parallel to the crack face. Later it was shown by Cotterell and Rice [4] that T-stress plays a vital role in directional stability of the crack paths. They showed that the directional instability is more likely to happen in a positive T-stress field. The popularity of using the T-stress as the second parameter is not limited to the above examples. Betegon and Hancock [5], O'Dowd and Shih [6] and Ayatollahi et al [7] used the two-parameter approach to characterize the elastic-plastic field. They found in a cracked specimen where the T-stress has a negative value the normal stress field ahead of the crack tip is not fully characterized by the HRR field. On the other hand in cracked specimen where the T-stress does not exist or it has a positive value the stress field can be estimated by the HRR approach.

Hancock et al [8], investigated the effect of T-stress on the fracture toughness of materials. Different specimens (centre cracked, single edge cracked and three point bending specimens) made from the same material were used. It was revealed that the plane strain toughness in different geometries is considerably different. They found that the geometries which show a positive T-stress (such as single edge crack or compact tension specimens) exhibit a geometry independent toughness. On the other hand a negative T-stress, which occurs in centre cracked specimens, makes the toughness dependent to the geometry of the specimen and increases the toughness compared to zero or positive T-stress levels. Apart from the aforementioned examples, T-stress is also influential in the crack growth rate, crack tunneling and the size of plastic zones [9; 10].

T-stress determination

To determine the T-stress numerically many different methods have been proposed in different types of specimens. These include the stress substitution, variational formulation, Eshelby J integral, interaction integral, line spring and weight function methods [11]. However, the accuracy of these numerical techniques depend on geometry or mesh refinement and are only applicable to specific configurations. Therefore, the need is evident to have a robust experimental technique to determine the T-stress in order to validate simulations.

Despite the importance of the T-stress, the experimental work to determine the T-stress is very limited. Only recently Maleski et al [12] used strain gauges to determine the T-stress in mode I loading condition. They used the Williams' solution and investigate using two or three terms of the expansion. Data was collected from one and two strain gauges respectively bonded at 60 and 120 degree from crack face and away from area where out of plane displacement exist. Their technique was only validated in mode I conditions. The position of the strain gauges will change with respect to the crack face as the crack grow or kink and the sensitivity of this technique to the gauge position makes the results unrealistic.

Inspired by the fact that in recent years Thermoelastic Stress Analysis (TSA) has proved to be an ideal technique for the determination of mode I, II and mixed stress intensity factors [13; 14], Zanganeh et al [15] have developed a technique to determine the T-stress from TSA images. They also developed a technique to determine the T-stress in pure mode I loading conditions [16]. The purpose of this work is to determine the T-stress in mixed mode conditions using finite element and TSA and DIC experimental techniques.

Methodology

As is well known, under adiabatic and reversible conditions the thermoelastic signal, S, is proportional to the variation of the sum of the principal stresses. Assuming plane stress conditions the sum of the principal stresses can be written based on Williams' solution as a series expansion,

$$AS = \Delta(\sigma_{xx} + \sigma_{yy}) = \sum_{n=0}^{\infty} 2nr^{\frac{n}{2}-1}\left\{\Delta a_n \cos\left[\left(\frac{n}{2}-1\right)\theta\right] - \Delta b_n \sin\left[\left(\frac{n}{2}-1\right)\theta\right]\right\}. \quad (1)$$

where, A is the thermoelastic calibration factor, σ_{xx} and σ_{yy} are stresses in x and y directions, respectively. r and θ are distance and angle from crack tip to the point of interest as shown in Figure 1.

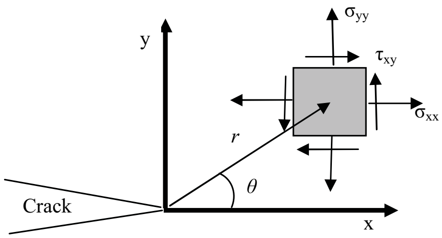

Figure 1 - Stress distribution ahead of a crack

a and b are constants which are proportional to the stress intensity factors and the T-stress using equation 2.

$$K_I = \frac{a_1}{\sqrt{2\pi}},\ K_{II} = \frac{-b_1}{\sqrt{2\pi}} \text{ and } T = 4a_2. \quad (2)$$

in which K_I is mode I stress intensity factor, K_{II} is mode II stress intensity factor and T is the T-stress. Since the number of data points obtained from a TSA image is always more than twice of the number of terms usually used in the expansion, equation (1) forms an over-determined system of equations. By solving equation 1 and using equation 2 intensity factors and the T-stress can be determined.

The output of DIC technique is the displacement field. Similarly, the Williams' displacement field ahead a crack tip was used to determine the *a* and *b* parameters to find the intensity factors and T-stress.

Experiments

In the first stage, pure mode I loading conditions were created ahead of a 4mm notch in a 5mm thick DCB specimen with the dimensions shown in Figure 2. The specimen was machined from a plate 7010 T7651 aluminium alloy and spark eroded to introduce the notch into the specimen.

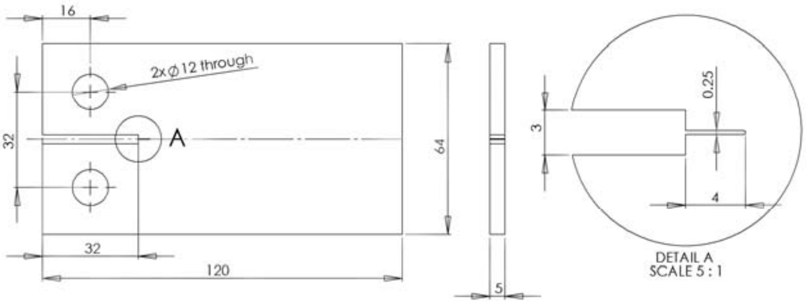

Figure 2 - Specimen dimension in mm

Both TSA and DIC techniques were used to determine the stress intensity factor and T-stress in this type of specimen. Figure 3 shows a typical result gained from TSA and DIC for a DCB specimen.

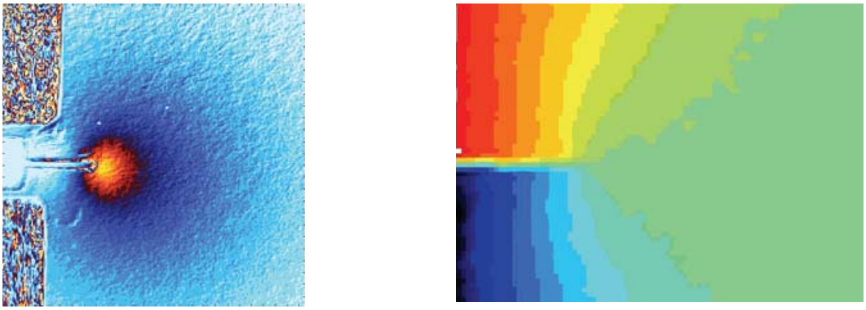

(a) (b)

Figure 3 - Typical a) sum of principal stress gained from TSA b)Vertical displacement gained from DIC for a DCB speciemn

A 100kN MAND hydraulic test machine was used to load the specimen. A load ranges of 0.5kN to 1.5kN with the frequency of 20Hz was applied to the specimen during capturing the image for TSA and the same load range in 0.15Hz was applied during the DIC capturing time. A Deltatherm 1410 camera was used to capture the thermoelastic signal from the surface of the specimen. In DIC analysis a 14 bit, 1600x1200 CCD camera and a Nikon lens with the resolution of 18.75 microns were used to record the images. DaVis software [17] was employed to correlate the images. The software was set up to use a 64x64 pixels interrogation window, followed by two iterations using a 32x32 pixels interrogation window with 50% overlap.

Results were analyzed using the methodology explained in previous section and the T-stress as well as intensity factors were calculated as shown in Figure 4.

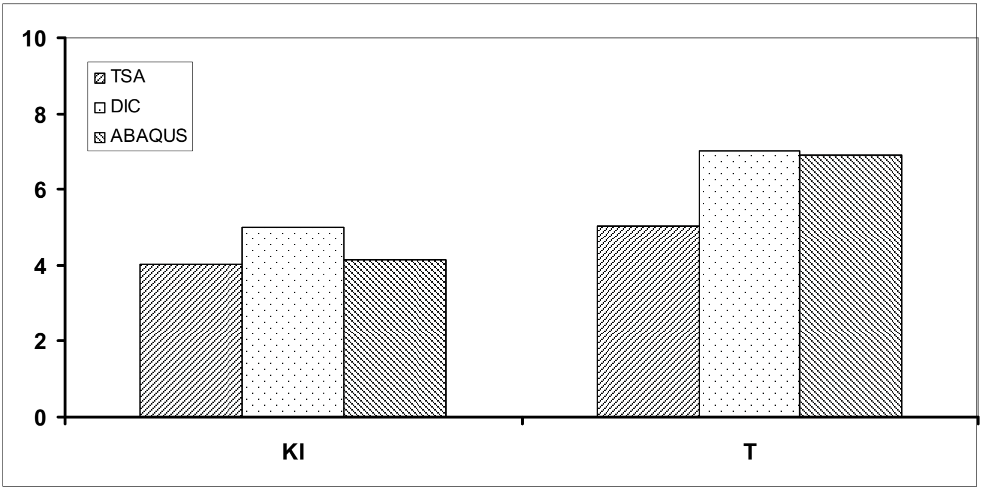

Figure 4 - Comparison of KI and T-stress for TSA, DIC and ABAQUS

As it was expected the K_{II} values were practically zero for this type of specimen so they have not been included in Figure 4. It is observed from Figure 4 that all TSA, DIC and ABAQUS [18] are in an acceptable range of agreement with each other. In this case the calculated mode I intensity factor from TSA and ABAQUS match better and DIC predict a higher intensity factor, however, for the T-stress, DIC result is closer to the ABAQUS simulation and TSA results is less than the other two approaches.

In the next stage, a centrally cracked specimen with the dimensions shown in Figure 5 was loaded under different loading angles ranging from 0 degree (pure mode I) to 90 degree (pure mode II). The same surface preparation and resolution as first stage (DCB specimen test) were used. In each loading angle 0.5kN to 10kN load range at 20Hz was applied during TSA data capture and 0.5 to 10kN load range at 0.15Hz was applied during DIC data capture. First, the images were recorded using DIC and the specimen was removed and the surface was painted matt black to be usable in TSA analysis. After doing the experiments for all the angles the same procedure as the first stage was performed to determine the T-stress.

In order to numerically simulate the problem, an elastic model as shown in Figure 6(a) was used in ABAQUS. In this model the load and boundary conditions have applied in such a way that the stress field ahead of both left and right crack tip are the same. A comparison between FE and experimental results is shown in Figure 7.

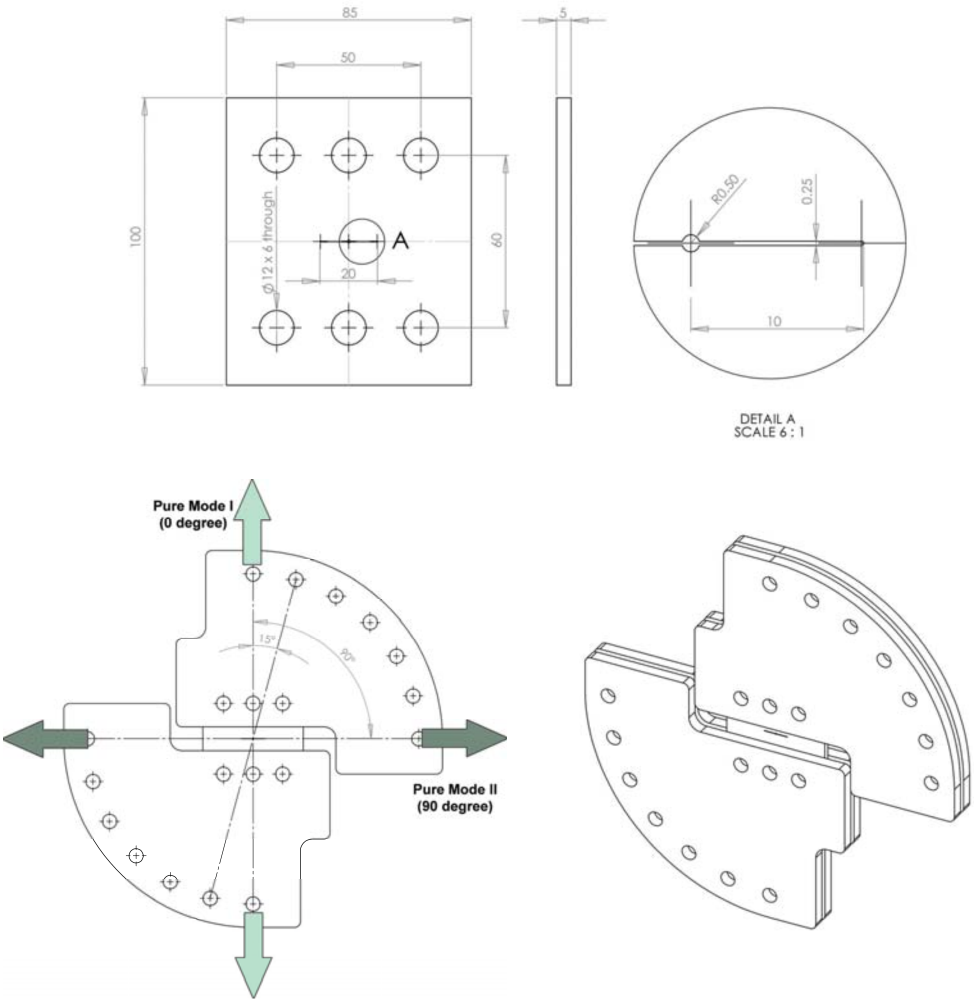

Figure 5 - Centrally cracked specimen and mixed mode grips

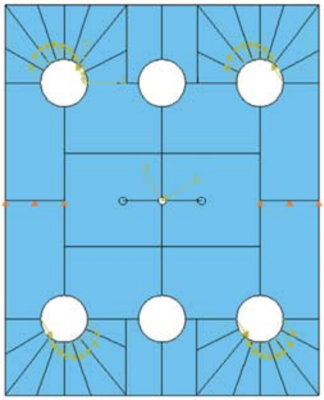
(a)

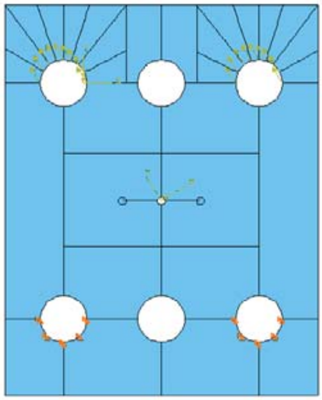
(b)

Figure 6 - ABAQUS model used for FEM simulation a) symmetric b) non-symmetric

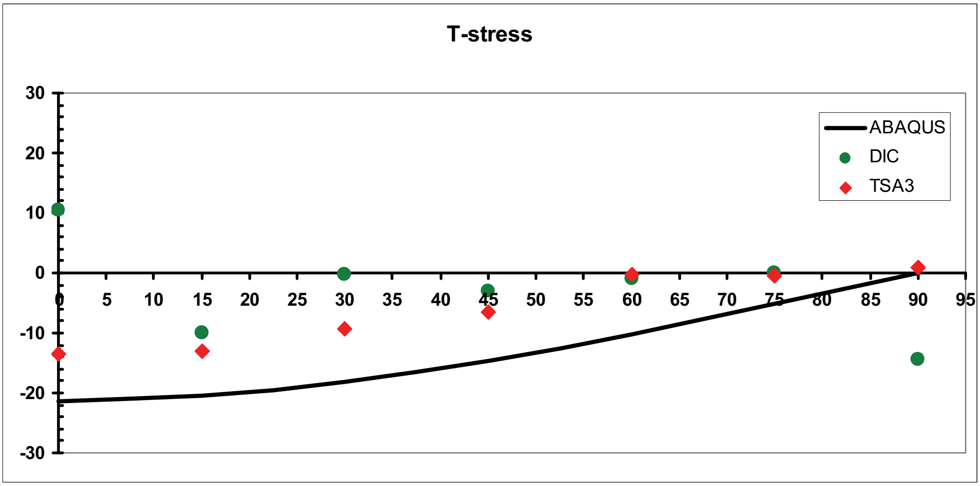

Figure 7 - Comparison of T-stress obtained from ABAQUS, DIC and TSA for the righthand crack

Discussion

It is observed from Figure 7 that there is reasonable agreement between the TSA and DIC calculated results in most of the angles. Apparently the calculated T-stress in pure mode I and II using DIC outlay the expected trend for the results. This might be due to a poor correlation in processing the results especially in the mode II case. Although the TSA and DIC agree with each other in most of the angles, they do not match the results predicted by ABAQUS. To investigate this matter another FE model was used to simulate the problem. In this model, Figure 6(b), a more realistic model was used such that the bottom boundary of the model, where the pins are mounted, were fixed. This introduces an eccentricity in the model which causes a different stress field ahead of the left and right crack tips. Results of this simulation are shown in Figure 8.

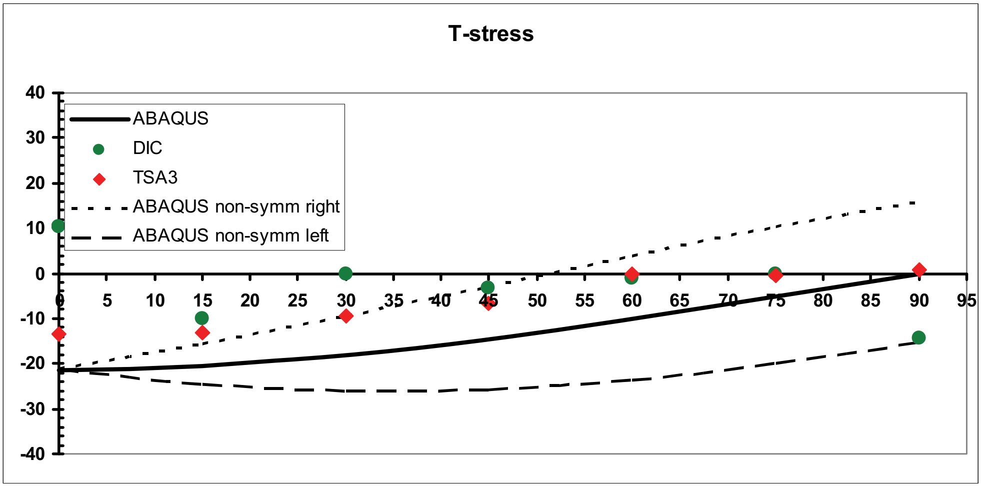

Figure 8 - Effect of non-symmetric or eccentric loading on ABAQUS calculated T-stress righthand crack

As it is observed from Figure 8, the T-stress results obtained from non-symmetric model used in ABAQUS vary in a broad range. In this case the experimental results are closer to the numerical results. It is evident that boundary condition and the eccentricity that may be introduced in the experiments are crucial in determined T-stresses using FEM. Regarding the fact that as experienced before [19], this type of mixed mode grips makes the specimen over-determined the eccentricity in loading is inevitable. Since these eccentricities stem from manufacturing inaccuracies which can not be simulated easily, the FE results are not entirely reliable and they can only be used to estimate the trend of the results especially in this case where two other experimental techniques are consistent with each other.

Conclusion

T-stress was determined in both pure mode I using DCB specimen and in mixed mode conditions in a centre cracked specimen under various loading angles. T-stresses were obtained numerically using FEM and experimentally using TSA and DIC. In pure mode I case experimental and FE results agreed. However, in mixed mode conditions in spite of agreement observed in experimental results, FE results were much higher than experimental results. It was shown that this disagreement is due to loading eccentricities which introduce during the experiment because of inaccuracies in manufacturing the grips and specimens.

References

[1] M.L. Williams: J. App. Mech. 24 (1957) 109–114.

[2] S.G. Larsson, and A.J. and Carlsson: J. Mech. Phys. Solids 21 (1973) 263–277.

[3] J.R. Rice: J Mech Phys Solids 22 (1974) 17-26.

[4] B. Cotterell, and J.R. and Rice: Int. J. Fracture 16 (1980) 155-169.

[5] C. Betegon, and J.W. and Hancock: J Appl Mech 58 (1991) 104-110.

[6] N.P. O'Dowd, and C.F. and Shih: J Mech Phys Solids 39 (1991) 989-1015.

[7] M.R. Ayatollahi, D.J. Smith, and M.J. and Pavier: Int. J. Fracture 113 (2002) 153-173.

[8] J.W. Hancock, W.G. Reuter, and D.M. and Parksin, in: E.M. Hackett, K.H. Schwalbe, and R.H. and Dodds, (Eds.), Constraint effects in fracture, ASTM STP 1171, 1993.

[9] L.G. Zhao, J. Tong, and J. and Byrne: Int. J. Fracture 109 (2001) 209-225.

[10] J. Tong: Eng. Fract. Mech. 69 (2002) 1325-1337.

[11] A.H. Sherry, C.C. France, and M.R. and Goldthor: Fatigue Fract. Engng. Mater. Struct. 18 (1995) 141-155.

[12] M.J. Maleski, M.S. Kirugulige, and H.V. and Tippur: Exp. Mech. 44 (2004) 522-532.

[13] F.A. Diaz, E.A. Patteson, R.A. Tomlinson, and J.R. and Yates: Fatigue Fract. Engng. Mater. Struct. 27 (2004) 571-583.

[14] J.R. Yates, M. Zanganeh, R.A. Tomlinson, M.W. Brown, and F.A. and Diaz: Eng. Fract. Mech. 75 (2008) 319-330.

[15] M. Zanganeh, R.A. Tomlinson, and J.R. and Yates: J Strain Anal. in press.

[16] M. Zanganeh, R.A. Tomlinson, and J.R. and Yates, in: SEM XI International Congress & Exposition on Experimental and Applied Mechanics, Orlando, Florida, USA, 2008.

[17] LaVision GmbH. www.lavision.de.

[18] ABAQUS/CAE V 6.6. http://www.simulia.com/products/abaqus_cae.html.

[19] Private communication with Dr C. Pinna, 2007.